









# Right ventricular to pulmonary artery coupling and outcome in patients with cardiac amyloidosis

Daniela Tomasoni <sup>1</sup>, Marianna Adamo <sup>1</sup>, Aldostefano Porcari<sup>2</sup>, Alberto Aimo <sup>3,4</sup>, Giovanni Battista Bonfioli<sup>1</sup>, Vincenzo Castiglione <sup>3,4</sup>, Maria Franzini<sup>5</sup>, Riccardo Maria Inciardi<sup>1</sup>, Anas Khalil<sup>3</sup>, Carlo Mario Lombardi<sup>1</sup>, Laura Lupi <sup>1</sup>, Matilde Nardi<sup>1</sup>, Chiara Oriecua<sup>6,7</sup>, Matteo Pagnesi <sup>1</sup>, Giorgia Panichella<sup>3</sup>, Maddalena Rossi<sup>2</sup>, Nicola Saccani <sup>1</sup>, Claudia Specchia<sup>7</sup>, Giuseppe Vergaro<sup>3,4</sup>, Marco Merlo <sup>2</sup>, Gianfranco Sinagra<sup>2</sup>, Michele Emdin<sup>3,4</sup>, and Marco Metra <sup>1\*</sup>

<sup>1</sup>Cardiology, ASST Spedali Civili di Brescia and Department of Medical and Surgical Specialties, Radiological Sciences, and Public Health, University of Brescia, Piazzale Spedali Civili, Brescia 25123, Italy; <sup>2</sup>Department of Cardiovascular, Azienda Sanitaria Universitaria Integrata Giuliano Isontina, University of Trieste, Trieste, Italy; <sup>3</sup>Health Science Interdisciplinary Center, Scuola Superiore Sant'Anna, Pisa, Italy; <sup>4</sup>Cardiology and Cardiovascular Medicine Division, Fondazione Toscana Gabriele Monasterio, Pisa, Italy; <sup>5</sup>Dipartimento di Ricerca Traslationale e delle Nuove Tecnologie in Medicina e Chirurgia, Università di Pisa, Pisa, Italy; <sup>6</sup>Department of Clinical and Experimental Sciences, University of Brescia, Brescia, Italy; and <sup>7</sup>Department of Molecular and Translational Medicine, University of Brescia, Brescia, Italy

Received 30 December 2022; accepted 20 May 2023; online publish-ahead-of-print 28 June 2023

## Aims

To investigate the prognostic value of the right ventricle-to-pulmonary artery (RV-PA) coupling in patients with either transthyretin (ATTR) or immunoglobulin light-chain (AL) cardiac amyloidosis (CA).

## Methods and results

Overall, 283 patients with CA from 3 Italian high-volume centres were included (median age 76 years; 63% males; 53% with ATTR-CA, 47% with AL-CA). The RV-PA coupling was evaluated by using the tricuspid annular plane systolic excursion/pulmonary artery systolic pressure (TAPSE/PASP) ratio. The median value of TAPSE/PASP was 0.45 (0.33–0.63) mm/mmHg. Patients with a TAPSE/PASP ratio <0.45 were older, had lower systolic blood pressure, more severe symptoms, higher cardiac troponin and N-terminal pro-B-type natriuretic peptide levels, greater left ventricular (LV) thickness, and worse LV systolic and diastolic function. A TAPSE/PASP ratio <0.45 was independently associated with a higher risk of all-cause death or heart failure (HF) hospitalization [hazard ratio (HR) 1.98, 95% confidence interval (CI) 1.32–2.96;  $P = 0.001$ ] and all-cause death (HR 2.18, 95% CI 1.31–3.62;  $P = 0.003$ ). The TAPSE/PASP ratio reclassified the risk of both endpoints [net reclassification index 0.46 (95% CI 0.18–0.74)  $P = 0.001$  and 0.49 (0.22–0.77)  $P < 0.001$ , respectively], while TAPSE or PASP alone did not (all  $P > 0.05$ ). The prognostic impact of the TAPSE/PASP ratio was significant both in AL-CA patients (HR for the composite endpoint 2.47, 95% CI 1.58–3.85;  $P < 0.001$ ) and in ATTR-CA (HR 1.81, 95% CI 1.11–2.95;  $P = 0.017$ ). The receiver operating characteristic curve showed that the optimal cut-off for predicting prognosis was 0.47 mm/mmHg.

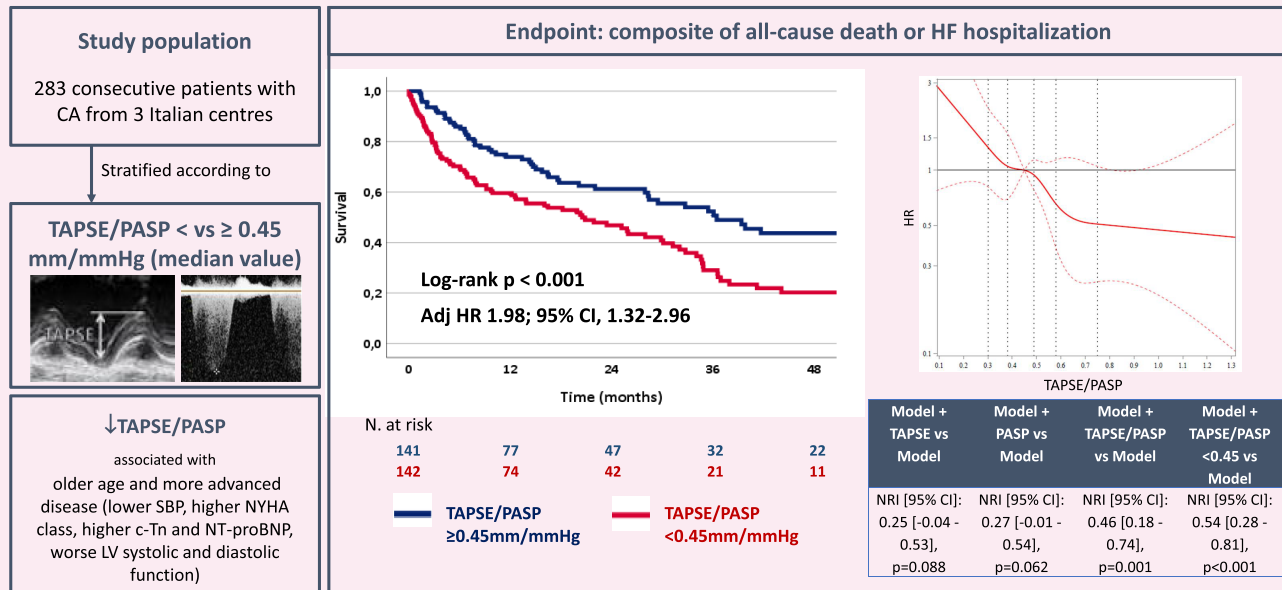
## Conclusion

In patients with CA, RV-PA coupling predicted the risk of mortality or HF hospitalization. The TAPSE/PASP ratio was more effective than TAPSE or PASP in predicting prognosis.

\* Corresponding author. E-mail: metramarco@libero.it

## Graphical Abstract

## Right ventricular to pulmonary artery coupling and outcome in patients with cardiac amyloidosis



## Keywords

cardiac amyloidosis • TAPSE/PASP • right ventricular to pulmonary artery coupling • right ventricular function • heart failure • prognosis

## Introduction

Cardiac amyloidosis (CA) is characterized by extracellular deposition of misfolded proteins, most commonly transthyretin (ATTR-CA) or immunoglobulin light-chains (AL-CA), leading to increased biventricular wall thickness and myocardial stiffness, typically with preserved left ventricular ejection fraction (LVEF).<sup>1-5</sup> CA is associated with increased left atrial pressure, which can be transmitted to the pulmonary vasculature, resulting in pulmonary hypertension (PH) and right ventricular (RV) remodelling.

RV dysfunction and PH have been reported as important prognostic factors in patients with CA.<sup>6,7</sup> The tricuspid annular plane systolic excursion/pulmonary artery systolic pressure (TAPSE/PASP) ratio is a non-invasively measured index of RV-to-pulmonary-circulation coupling, correlating with invasively evaluated RV systolic elastance and pulmonary arterial elastance.<sup>8-10</sup> The coupling between RV function and its afterload may provide a more comprehensive information about right heart performance than either TAPSE or PASP alone.<sup>9,11</sup>

Previous studies showed the prognostic significance of the TAPSE/PASP ratio in patients with heart failure (HF) regardless of LVEF.<sup>9,12-16</sup> To our knowledge, limited evidence is available about its prognostic role in patients with CA. The aim of this analysis was to investigate for the first time the prognostic value of non-invasive RV-pulmonary artery (PA) coupling, evaluated using the TAPSE/PASP ratio, in patients with CA.

## Methods

### Study population

We retrospectively evaluated consecutive patients diagnosed with AL- or ATTR-CA from 2011 to 2021 at three Italian high-volume centres:

Cardiology, ASST Spedali Civili and University of Brescia, Brescia ( $n = 139$ ); Cardiology Department, Fondazione Toscana Gabriele Monasterio, Pisa ( $n = 120$ ); Cardiovascular Department, Azienda Sanitaria Universitaria Integrata, Trieste ( $n = 24$ ). CA was diagnosed when AL or ATTR amyloid was demonstrated on tissue specimens from endomyocardial biopsy, or when there was imaging evidence of cardiac involvement plus tissue amyloid in a peripheral tissue biopsy (as suggested by current recommendations).<sup>1,17,18</sup>

After 2016, ATTR-CA was diagnosed non-invasively in patients with an intense myocardial uptake of bone tracers (Perugini Scores 2 and 3) and no monoclonal protein. Detailed data regarding CA diagnosis in this population have been previously published.<sup>3</sup> Patient data including demographics, medical history, physical examination, laboratory and echocardiographic findings, and treatment were extracted from electronic health records. According to routine clinical practice, follow-up was performed twice a year and some patients were lost during follow-up. Out of 356 patients, 73 (21%) with data missing for TAPSE and/or PASP values were excluded. A comparison of the study population vs. patients with missing data is provided in [Supplementary data online, Table S1](#). This study complied with the Declaration of Helsinki and was approved by the ethics committee of each centre. Patients did not give informed consent, since it was not possible nor was it deemed necessary in this retrospective electronic health record review.

### Echocardiographic measurements

Echocardiographic measurements were performed by trained cardiac sonographers in agreement with the American Society of Echocardiography and the European Association of Cardiovascular Imaging recommendations.<sup>19</sup> TAPSE was tracked in the RV-focused apical four-chamber view using M-mode echocardiography. PASP (mmHg) was calculated as follows:

$$4 \times [\text{peak velocity of TR}]^2 + [\text{estimated right atrial pressure}]$$

The estimated right atrial pressure is based on the inferior vena cava diameter and collapsibility. Patients without any noticeable tricuspid regurgitation (TR) signal or lacking either inspiratory/expiratory phases of inferior vena cava diameters were excluded.

## Study endpoints

The primary outcome of the study was the composite of all-cause death or HF hospitalization. The secondary outcome was all-cause death. We also evaluated cardiovascular death and HF hospitalization as separate endpoints (see [Supplementary data online](#)). HF hospitalizations were defined as an admission to hospital for symptoms of HF with the need for intravenous diuretic therapy. Data regarding outcome were collected during follow-up using electronic health records, chart review, and patient reporting or phone calls to patients or relatives.

## Statistical analysis

Normal distribution of continuous variables was explored through the Shapiro–Wilk test. Continuous variables were reported as mean  $\pm$

standard deviation (SD) or median and the interquartile range, whereas categorical variables were reported as absolute numbers and percentages. The relationship between TAPSE and PASP is shown in [Supplementary data online, Figure S1](#). We stratified the population according to the median value of the TAPSE/PASP ratio. Continuous variables were compared using the Student's *t*-test or Kruskal–Wallis test, and categorical variables were compared using the Pearson  $\chi^2$  test. The clinical endpoints were assessed with the Kaplan–Meier method and compared with the log-rank test. The prognostic impact of the TAPSE/PASP ratio on the primary composite endpoint and on all-cause mortality was evaluated by means of univariable and multivariable analyses. The number of variables entered into the Cox regression model was limited according to the number of events, based on the principle of not having more than 1 variable every 10 events for the primary composite endpoint. A total of 15 variables were entered into the multivariable model. These variables were associated with an increased risk of the composite endpoint at univariate analysis (*P*-value <0.05) and/or unbalanced between the two groups: age, AL vs. ATTR amyloidosis, New York Heart Association (NYHA) functional class, previous HF hospitalization, history of atrial fibrillation, systolic blood pressure (SBP),

**Table 1** Baseline clinical characteristics of the study population stratified by TAPSE/PASP ratio

Variable	All (N = 283)	TAPSE/PASP <0.45 mm/mmHg (N = 142)	TAPSE/PASP $\geq$ 0.45 mm/mmHg (N = 141)	P value
Clinical characteristics				
Age (years)	76 (69–82)	78 (71–84)	75 (66–80)	<b>0.001</b>
Sex males, n (%)	177 (63)	95 (67)	82 (58)	0.129
BMI (kg/m <sup>2</sup> )	25 (23–28)	25 (22–28)	25 (23–28)	0.427
SBP (mmHg)	120 (110–139)	117 (105–132)	125 (110–140)	<b>0.009</b>
DBP (mmHg)	70 (60–80)	70 (60–78.8)	70 (65–80)	0.066
HR (bpm)	70 (62–81)	70 (61–80)	72 (63–83)	0.285
Type of amyloidosis				<b>0.004</b>
ATTR, n (%)	151 (53)	88 (62)	63 (45)	
AL, n (%)	132 (47)	54 (31)	78 (55)	
Hypertension, n (%)	177 (63)	87 (61)	90 (64)	0.656
Dyslipidaemia, n (%)	109 (39)	53 (37)	56 (40)	0.679
Diabetes, n (%)	50 (18)	33 (23)	17 (12)	<b>0.014</b>
CAD, n (%)	50 (18)	29 (20)	21 (15)	0.223
COPD, n (%)	22 (8)	12 (0.08)	10 (0.07)	0.670
CKD, n (%)	120 (42)	61 (43)	59 (42)	0.850
History of atrial fibrillation, n (%)	130 (46)	88 (62)	42 (30)	<b>&lt;0.001</b>
Previous HF hospitalization, n (%)	145 (51)	87 (61)	58 (41)	<b>0.001</b>
NYHA class				<b>&lt;0.001</b>
I, n (%)	55 (19)	16 (11)	39 (28)	
II, n (%)	130 (46)	61 (43)	69 (50)	
III, n (%)	90 (32)	57 (41)	33 (22)	
IV, n (%)	8 (3)	8 (5)	0 (0)	
Angina, n (%)	37 (13)	20 (14)	17 (12)	0.613
Asthenia, n (%)	65 (23)	40 (28)	25 (18)	<b>0.034</b>
Syncope, n (%)	37 (13)	19 (13)	18 (13)	0.878
PM/ICD, n (%)	43 (15)	27 (19)	16 (11)	0.116

Values are reported as means  $\pm$  SDs or medians (interquartile ranges). Bold characters indicate statistical significance (*P*-value <0.05).

AL, light-chain amyloidosis; ATTR, transthyretin amyloidosis; BMI, body mass index; CAD, coronary artery disease; CKD, chronic kidney disease; COPD, chronic obstructive pulmonary disease; DBP, diastolic blood pressure; HF, heart failure; HR, heart rate; ICD, implantable cardioverter/defibrillator; NYHA, New York Heart Association; PM, pacemaker; SBP, systolic blood pressure, TAPSE/PASP, tricuspid annular plane systolic excursion/pulmonary artery systolic pressure.

**Table 2** Laboratory and echocardiographic findings of the study population stratified by TAPSE/PASP ratio

	All (N = 283)	TAPSE/PASP <0.45 mm/mmHg (N = 142)	TAPSE/PASP ≥0.45 mm/mmHg (N = 141)	P value
<b>Laboratory findings</b>				
Haemoglobin (g/dL)	12.5 ± 1.7	12.5 ± 1.7	12.4 ± 1.8	0.670
White blood cell count (μL)	4173 ± 3914	3418 ± 3590	4982 ± 4095	<b>0.001</b>
eGFR (mL/min)	53 (38–76)	50 (37–71)	58 (41–78)	0.104
Aspartate transaminase (u/L)	27 (19–32)	23 (19–32)	23 (18–32)	0.263
Alanine aminotransferase (u/L)	21(15–30)	21 (16–31)	19 (15–29)	0.142
Gamma-glutamyl transpeptidase (u/L)	41 (21–98)	50 (27–122)	30 (19–74)	<b>0.009</b>
INR	1.1 (1.0–1.3)	1.2 (1.1–1.5)	1.1 (1–1.2)	<b>&lt;0.001</b>
Lactate dehydrogenase (u/L)	317 ± 167	345 ± 197	282 ± 115	<b>0.007</b>
NT-proBNP (ng/L)	3033 (1099–7587)	4693 (2631–10011)	1804 (626–3726)	<b>&lt;0.001</b>
hs-Tn (ng/L)	43 (26–75)	54 (35–77)	31 (21–61)	<b>&lt;0.001</b>
<b>Echocardiographic findings</b>				
LVEF (%)	55 (50–61)	53 (50–59)	58 (53–64)	<b>&lt;0.001</b>
IVS (mm)	16 (14–19)	17 (15–20)	15 (13–17)	<b>&lt;0.001</b>
LVPW (mm)	14 (12–16)	15 (13–17)	13 (11–15)	<b>&lt;0.001</b>
LVEDD (mm)	45 (41–50)	45 (40–49)	46 (42–52)	0.070
LVESD (mm)	30 (27–34)	31 (28–34)	30 (26–34)	0.082
LVMI (g)	159 (127–226)	175 (133–255)	151 (115–190)	<b>&lt;0.001</b>
LV-GLS (%)	−12.9±−4.7	−11.5 ± −4.0	−14.3±−4.9	<b>&lt;0.001</b>
Medial S' (cm/s)	6 (4–7)	5 (3–6)	7 (5–8)	<b>&lt;0.001</b>
Lateral S' (cm/s)	6 (5–8)	5 (4–7)	7 (5–8)	<b>&lt;0.001</b>
E/A	1.2 (0.8–2.2)	2.1 (1.5–2.8)	1.0 (0.7–1.3)	<b>&lt;0.001</b>
EDT (ms)	182 (150–219)	168 (140–200)	207 (165–243)	<b>&lt;0.001</b>
E/e'	15 (11–19)	17 (14–23)	13 (10–17)	<b>&lt;0.001</b>
LA diameter (mm)	45 (40–48)	46 (43–49)	43 (37–47)	<b>&lt;0.001</b>
LA area (cm <sup>2</sup> )	27.0 ± 8.5	29.5 ± 5.5	24.7 ± 10.0	<b>&lt;0.001</b>
LAVI (mL/m <sup>2</sup> )	44 (35–52)	48 (41–56)	40 (29–49)	<b>&lt;0.001</b>
Moderate to severe MR, n (%)	43 (15)	28 (20)	15 (11)	<b>0.033</b>
RA volume (mL)	57 ± 29	72 ± 27	48 ± 25	<b>0.002</b>
TAPSE (mm)	18.0 ± 4.9	14.9 ± 3.6	21.33 ± 3.8	<b>&lt;0.001</b>
s' TDI (cm/s)	11 ± 3	10 ± 2.7	12.8 ± 3	<b>&lt;0.001</b>
FAC (%)	39 (33–44)	35 (30–42)	42 (37–46)	<b>0.001</b>
RV dilatation, n (%)	42 (15)	34 (24)	8 (6)	<b>&lt;0.001</b>
RV wall thickness (mm)	8.3 ± 2.1	9.1 ± 1.8	7.7 ± 2.1	<b>&lt;0.001</b>
PASP (mmHg)	38 (32–46)	45 (40–52)	33 (29–36)	<b>&lt;0.001</b>
TAPSE/PASP (mm/mmHg)	0.45 (0.33–0.63)	0.33 (0.28–0.38)	0.63 (0.53–0.76)	<b>&lt;0.001</b>
IVC diameter during expiration (mm)	19 (16–23.5)	22 (18–25)	17 (14–20)	<b>&lt;0.001</b>
Pericardial effusion, n (%)	112 (40)	59 (42)	53 (38)	0.156

Values are reported as means ± SDs or medians (interquartile ranges). Bold characters indicate statistical significance (*P*-value <0.05).

EDT, E wave deceleration time; eGFR, estimated glomerular filtration rate; FAC, fractional area change; hs-Tn, high-sensitivity troponin; INR, international normalized ratio; IVC, inferior vena cava; IVS, interventricular septum; LA, left atrium; LAVI, left atrium volume index; LVEDD, left ventricular end-diastolic diameter; LVEF, left ventricular ejection fraction; LVESD, left ventricular end-systolic diameter; LV-GLS, left ventricular global longitudinal strain; LVMI, left ventricular mass index; LVPW, left ventricular posterior wall; MR, mitral regurgitation; NT-proBNP, N-terminal pro-B-type natriuretic peptide; PASP, pulmonary artery systolic pressure; RA, right atrium; RV, right ventricle; TAPSE, tricuspid annular plane systolic excursion; TDI, tissue doppler imaging.

N-terminal pro-B-type natriuretic peptide (NT-proBNP), high-sensitivity troponin T (hs-TnT), estimated glomerular filtration rate, LVEF, left ventricular global longitudinal strain (LV-GLS), and RV dilatation.

Sex was also added to the model. A further model is presented in [Supplementary data online](#) including additive meaningful echocardiographic parameters (i.e. left ventricular mass index, E/e' ratio, and left atrial volume

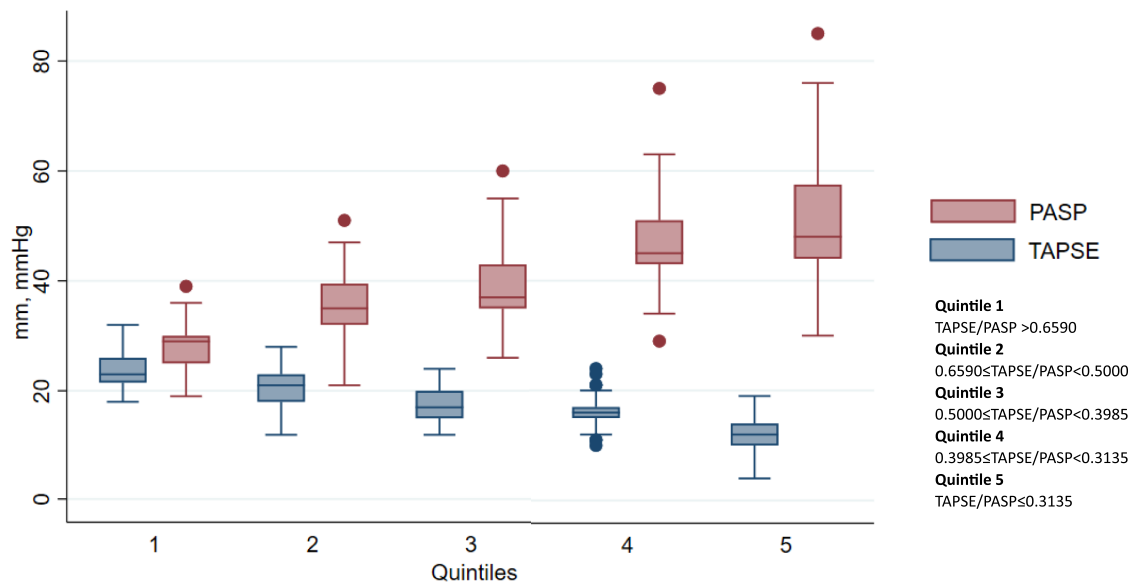


**Figure 1** Box plots reporting TAPSE and PASP values stratified by quintiles.

**Table 3** Medical treatment and outcome of the study population stratified by TAPSE/PASP ratio

Variable	All (N = 283)	TAPSE/PASP <0.45 mm/mmHg (N = 142)	TAPSE/PASP ≥0.45 mm/mmHg (N = 141)	P value
<b>Treatment</b>				
ASA, n (%)	83 (31)	37 (27)	46 (34)	0.235
ACEi, n (%)	89 (33)	49 (36)	40 (30)	0.244
ARBs, n (%)	48 (18)	19 (14)	29 (21)	0.111
ARNI, n (%)	4 (1.5)	2 (1.5)	2 (1.5)	1.000
Beta-blockers, n (%)	161 (60)	92 (68)	69 (51)	<b>0.004</b>
Mineralocorticoids, n (%)	119 (41)	64 (47)	46 (34)	<b>0.026</b>
Direct oral anticoagulants, n (%)	74 (27)	44 (32)	30 (22)	0.061
VKA, n (%)	48 (18)	36 (26)	12 (9)	<b>&lt;0.001</b>
Furosemide, n (%)	194 (72)	115 (85)	79 (59)	<b>&lt;0.001</b>
Furosemide dose (mg)	50 (25–75)	50 (25–100)	25 (0–75)	<b>&lt;0.001</b>
<b>Outcomes</b>				
Death or HF hospitalization	159 (56)	98 (69)	61 (43)	<b>&lt;0.001</b>
Death, n (%)	126 (45)	77 (54)	49 (35)	<b>0.001</b>
CV death <sup>a</sup> , n (%)	38 (18)	30 (29)	8 (7)	<b>&lt;0.001</b>
HF hospitalization, n (%)	126 (45)	58 (41)	31 (22)	<b>0.001</b>

Bold characters indicate statistical significance ( $P$ -value <0.05).

ACEi, angiotensin converting enzyme inhibitor; ARBs, angiotensin receptor blockers; ARNI, angiotensin receptor neprilysin blocker; ASA, acetylsalicylic acid; CV, cardiovascular; HF, heart failure; VKA, vitamin K antagonist.

<sup>a</sup>The cause of death was not available for all patients (N missing = 70 patients).

index). Results of the Cox regression analyses are reported as unadjusted or adjusted hazard ratio (HR) and 95% confidence interval (CI). The best cut-off from receiver operating characteristic (ROC) curve was calculated through the Youden method. Additionally, departure from linearity in the relationship between TAPSE/PASP ratio (treated as a continuous variable)

and the hazard of experiencing a composite endpoint was investigated with a restricted cubic spline (RCS) model with knots at five evenly spaced percentiles (i.e. 16.6th, 33.3th, 50th, 66.6th, and 83.3th percentiles), adjusted for the same variables as above. Briefly, an RCS describes the relationship between a response variable and a continuous covariate using smoothly



joined piecewise cubic polynomials, which were restricted to be linear in the tails. The likelihood ratio test was used to determine whether the RCS model significantly increased the likelihood function compared with a simpler model that assumed a linear relationship. The net reclassification index (NRI) was used to assess the added value of the 0.45 mm/mmHg TAPSE/PASP cut-off and absolute TAPSE/PASP values to the prognostic model above. Statistical tests were based on a two-sided significance level of 0.05. Statistical analyses were performed using the SPSS software, version 21 (SPSS Inc., Chicago, IL, USA), SAS software, version 9.4 (SAS Institute, Cary, NC, USA), and R (version 3.4.4).

## Results

### Clinical characteristics

A total of 283 patients were included. Median age was 76 years (69–82), and 63% were male. ATTR-CA was diagnosed in 151 patients (53%) and AL-CA in 132 (47%). The median value of TAPSE/PASP ratio was 0.45 (0.33–0.63) mm/mmHg. Compared with patients with a TAPSE/PASP ratio  $\geq 0.45$  mm/mmHg, those with TAPSE/PASP ratio  $< 0.45$  mm/mmHg were older and with a higher prevalence of ATTR-CA. They also presented with lower SBP, more severe symptoms as assessed with NYHA functional class, and higher rates of coexisting atrial fibrillation or previous hospitalizations for HF. The prevalence of comorbidities was similar between groups (Table 1).

### Laboratory and echocardiographic findings

Patients with a TAPSE/PASP ratio  $< 0.45$  mm/mmHg had higher hs-TnT and NT-proBNP levels, greater left ventricular (LV) thickness, worse LV systolic and diastolic function, and more dilated atria. Furthermore, a TAPSE/PASP ratio  $< 0.45$  mm/mmHg was associated with greater RV hypertrophy and dilatation, and a worse RV function (Table 2). We also subdivided the study population in quintiles (see Supplementary data online, Table S2). Differences among the subgroups remained significant, with the lowest quintile (Quintile 5, i.e. TAPSE/PASP  $< 0.3135$ ) presenting the most advanced stage. Figure 1 reports the distribution of TAPSE and PASP across quintiles using the box plots.

### RV-PA uncoupling and outcome

During an 18-month median follow-up (7–38), the primary endpoint of all-cause death or HF hospitalization occurred in 159 patients (56.2%). A total of 126 patients (44.5%) died (Table 3). The hazard of experiencing a composite endpoint proportionally increased with the reduction of TAPSE/PASP values (Figure 2). The optimal cut-off for the prediction of the primary endpoint from the ROC curve was 0.47.

Patients with TAPSE/PASP  $< 0.45$  mm/mmHg presented a higher risk of the composite endpoint which occurred in 69 vs. 43% of the patients (HR 1.88, 95% CI 1.37–2.60;  $P < 0.001$ ) and all-cause death, occurring in 54 vs. 35% of the patients (HR 1.81, 95% CI 1.26–2.59;  $P < 0.001$ ) (Figure 3, Tables 3 and 4). The prognostic impact of TAPSE/PASP ratio was confirmed in the subgroups with either AL- or ATTR-CA, and it was more evident in AL-CA patients (HR for the composite endpoint 2.47, 95% CI 1.58–3.85;  $P < 0.001$  and HR 1.81, 95% CI 1.11–2.95;  $P = 0.017$  in AL- and ATTR-CA, respectively) (see Supplementary data online, Figures S2 and S3). The Kaplan–Meier curve for cardiovascular death and HF hospitalization as individual outcomes are reported in Supplementary data online, Figure S4 (log-rank  $P < 0.001$  and 0.001, respectively). After adjustment for other clinically relevant variables and/or variables associated with prognosis as reported in Methods section, TAPSE/PASP  $< 0.45$  mm/mmHg remained significantly associated with the risk of the composite endpoint (adjusted HR 1.98, 95% CI 1.32–2.96;  $P = 0.001$ ) and all-cause mortality (adjusted HR 2.18, 95% CI 1.31–3.62;  $P = 0.003$ ) (Tables 4 and 5, see Supplementary data online, Table S3).

**Table 4** Impact of TAPSE, PASP, and TAPSE/PASP ratio on the composite of all-cause death or HF hospitalization and all-cause death (univariate and multivariate COX model; NRI<sup>a</sup>)

Outcomes	TAPSE	PASP	TAPSE and PASP	TAPSE/PASP	TAPSE/PASP $< 0.45$ mm/mmHg (yes vs. no)
All-cause death or HF	Crude HR (95% CI), $P$ -value	1.02 (1.01 to 1.04), <b>0.001</b>		0.21 (0.09–0.47), <b>&lt;0.001</b>	1.88 (1.37 to 2.60), <b>&lt;0.001</b>
	Adjusted HR (95% CI), $P$ -value <sup>b</sup>	0.94 (0.90–0.97), <b>0.001</b>	1.02 (1.00 to 1.04), <b>0.028</b>	0.14 (0.05–0.40), <b>&lt;0.001</b>	1.98 (1.32 to 2.96), <b>0.001</b>
	NRI (95% CI), $P$ -value <sup>b</sup>	0.25 (–0.04 to 0.53), 0.088	0.27 (–0.01 to 0.54), 0.062	0.57 (0.32 to 0.86), <b>0.001</b>	0.54 (0.28 to 0.81), <b>&lt;0.001</b>
All-cause death	Crude HR (95% CI), $P$ -value	0.93 (0.90 to 0.96), <b>&lt;0.001</b>	1.02 (1.01 to 1.03), <b>0.010</b>	0.23 (0.09 to 0.56), <b>&lt;0.001</b>	1.81 (1.26 to 2.59), <b>&lt;0.001</b>
	Adjusted HR (95% CI), $P$ -value <sup>b</sup>	0.95 (0.91 to 0.99), <b>0.016</b>	1.02 (0.99 to 1.04), 0.170	0.15 (0.04 to 0.54), <b>0.004</b>	2.18 (1.31 to 3.62), <b>0.003</b>
	NRI (95% CI), $P$ -value <sup>b</sup>	0.25 (–0.04 to 0.53), 0.088	0.19 (–0.09 to 0.47), 0.193	0.46 (0.18 to 0.73), <b>0.001</b>	0.44 (0.17 to 0.72), <b>0.002</b>

HR for continuous variables (TAPSE, PASP, and TAPSE/PASP ratio) refers to each unit increase. Bold characters indicate statistical significance ( $P$ -value  $< 0.05$ ).

CI, confidence interval; HF, heart failure; HR, hazard ratio; NRI, net reclassification index; PASP, pulmonary artery systolic pressure; SBP, systolic blood pressure; TAPSE, tricuspid annular plane systolic excursion.

<sup>a</sup>NRI for the composite endpoint and for all-cause death was calculated adding TAPSE, PASP, TAPSE and PASP, and TAPSE/PASP to a standardized model.

<sup>b</sup>The model for multivariable analysis and NRI includes age, sex, type of amyloidosis, NYHA class, previous HF hospitalization, history of atrial fibrillation, NT-proBNP, hs-TnT, eGFR, LVEF, LV GL2Dstrain, RV dilatation, and SPB.

**Table 5** Multivariable model for the composite endpoint of all-cause death or HF hospitalization and for all-cause death

	All-cause death or HF hospitalization		All-cause death	
	HR (95% CI)	P-value	HR (95% CI)	P-value
Age (+1 year)	1.06 (1.03–1.08)	<0.001	1.07 (1.04–1.10)	<0.001
Sex (male vs. female)	1.24 (0.81–1.90)	0.315	1.29 (0.80–2.07)	0.304
AL vs. ATTR	3.70 (2.23–6.14)	<0.001	5.49 (3.08–9.78)	<0.001
History of HF	1.40 (0.95–2.06)	0.094	2.02 (1.24–3.28)	0.005
Atrial fibrillation	1.12 (0.67–1.87)	0.665	0.82 (0.45–1.49)	0.508
SBP	0.99 (0.98–1.01)	0.435	0.98 (0.97–0.995)	0.007
NYHA class	1.07 (0.81–1.41)	0.630	0.64–1.20	0.873
eGFR	0.99 (0.99–1.01)	0.668	0.99 (0.98–1.00)	0.047
NT-proBNP	1.00 (1.00–1.00)	0.530	1.001 (1.001–1.001)	0.004
hs-troponin	1.01 (1.004–1.009)	<0.001	1.01 (1.002–1.01)	0.001
LVEF	1.01 (0.98–1.03)	0.662	1.03 (0.997–1.06)	0.076
LV-GLS	0.98 (0.93–1.04)	0.541	1.04 (0.97–1.11)	0.248
RV dilatation	0.83 (0.46–1.51)	0.539	0.82 (0.63–1.43)	0.346
TAPSE (mm)	0.94 (0.90–0.97)	0.001	0.95 (0.91–0.99)	0.016
PASP (mmHg)	1.02 (1.00–1.04)	0.028	1.02 (0.99–1.04)	0.170
RV coupling				
TAPSE/PASP (mm/mmHg)	0.14 (0.05–0.40)	<0.001	0.15 (0.04–0.54)	0.004
TAPSE/PASP <0.45 mm/mmHg (yes vs. no)	1.98 (1.32–2.96)	0.001	2.18 (1.31–3.62)	0.003

Bold characters indicate statistical significance ( $P$ -value <0.05).

AL, light-chain amyloidosis; ATTR, transthyretin amyloidosis; eGFR, estimated glomerular filtration rate; HF, heart failure; hs-Tn, high-sensitivity troponin; LVEF, left ventricular ejection fraction; LV-GLS, left ventricular global longitudinal strain; NYHA, New York Heart Association; NT-proBNP, N-terminal pro-B-type natriuretic peptide; RV, right ventricular; SBP, systolic blood pressure; TAPSE/PASP, tricuspid annular plane systolic excursion/pulmonary artery systolic pressure.

As shown in *Figure 2*, the non-linear function failed to significantly improve the fit of the model ( $P = 0.649$ ). Therefore, we adopted the linear function to represent the relationship between TAPSE/PASP ratio and the hazard of experiencing a composite endpoint.

TAPSE and PASP as separate parameters were significantly related to clinical endpoints (*Tables 4 and 5, Figure 4*). However, when added to the model including prognostically relevant variables (see Methods section), both TAPSE/PASP <0.45 mm/mmHg [NRI (95% CI): 0.54 (0.28–0.81),  $P < 0.001$ ] and the absolute TAPSE/PASP values [NRI (95% CI): 0.46 (0.18–0.74)  $P = 0.001$ ] reclassified patient risk, while TAPSE or PASP alone did not (all  $P$ -value >0.05) (*Table 4*). [Supplementary data online, Figure S5](#) reports the integrated discrimination improvement and area under the curve (AUC).

## Discussion

This is the first study to investigate the role of RV-PA uncoupling in patients with CA. The main findings were the following: (i) a TAPSE/PASP ratio <0.45 mm/mmHg was independently associated with the risk of the composite outcome of all-cause death or HF hospitalization in patients with CA, with about two-fold increased risk; (ii) a TAPSE/PASP ratio <0.45 mm/mmHg was also associated with a higher risk of all-cause death, cardiovascular death, and HF hospitalization as individual endpoints; (iii) in patients with CA, a TAPSE/PASP ratio <0.45 mm/mmHg and the absolute TAPSE/PASP reclassified the risk better than TAPSE or PASP considered as separate parameters (*Graphical Abstract*).

Guazzi et al.<sup>8</sup> first proposed the TAPSE/PASP ratio as a non-invasive index of RV-PA coupling. Its correlation with invasive measures has

been validated in patients with severe PH.<sup>10</sup> The TAPSE/PASP ratio has also shown a strong association with outcome in HF patients irrespective of LVEF.<sup>12,13,20</sup> More recently, the prognostic impact of RV-PA coupling was confirmed in patients with HF and secondary mitral regurgitation<sup>16</sup> and in those with valvular heart disease undergoing percutaneous or surgical correction.<sup>14,15,21–24</sup> The majority of studies assigned the optimal cut-off for TAPSE/PASP by Cox proportional hazards, whereas some considered the median TAPSE/PASP ratio value of the overall population as the cut-off. As a consequence, the proportion of patients presenting RV-PA uncoupling and the cut-off values used in different populations are largely variable, between 0.28 and 0.55 mm/mmHg or even higher.<sup>22</sup> In the current study, we stratified the population according to the median TAPSE/PASP value (0.45 mm/mmHg). Nevertheless, using a ROC curve analysis, we found that the optimal cut-off for the prediction of the primary endpoint was TAPSE/PASP = 0.47 mm/mmHg, which was almost equal to the threshold previously reported in different settings.<sup>9,20</sup>

Nakagawa et al.<sup>20</sup> reported that RV-PA uncoupling, defined as TAPSE/PASP ratio <0.48 mm/mmHg, was associated with a 2.75-fold increased risk of the composite endpoint of all-cause death or HF hospitalization in a large cohort of patients with HF and preserved LVEF. CA may be considered as a specific cause of HF with preserved LVEF (HFpEF),<sup>3,25,26</sup> even if in the late stages LVEF tends to decrease. In a systematic review of screening studies, the prevalence of CA was 12% (95% CI 6–20%) in HFpEF ( $n = 6$  studies) and 10% (95% CI 6–15%) in HF with reduced or mildly reduced ejection fraction ( $n = 2$ ).<sup>27</sup> Its prevalence is also increasing due to recent advances in cardiac imaging and diagnostic strategies.<sup>1,2</sup> While broad data support the role of TAPSE/PASP in HF, limited data are available in

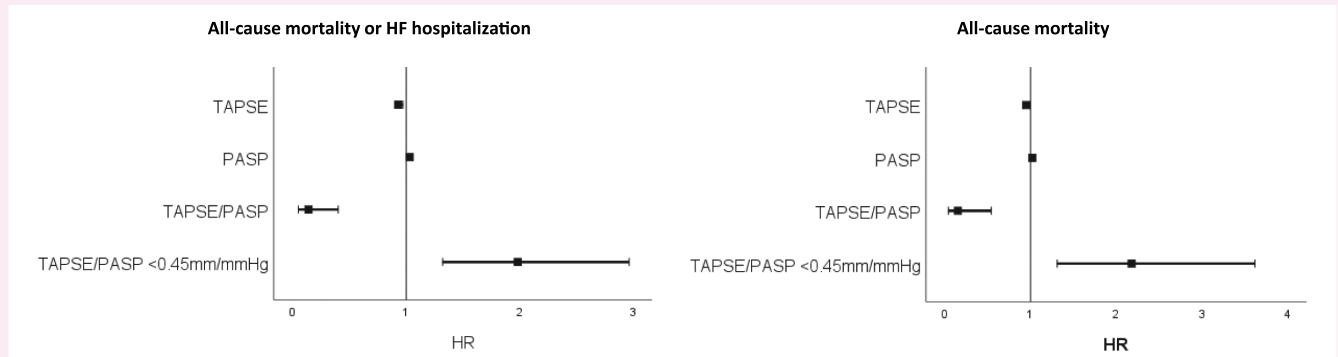


**Figure 4** Forest plot showing the prognostic role of TAPSE/PASP as a continuous variable, TAPSE/PASP <0.45 mm/mmHg and TAPSE or PASP as individual parameters (left panel: all-cause mortality or HF hospitalization; right panel: all-cause mortality) (multivariable analysis). HR for continuous variables (TAPSE/PASP, TAPSE, PASP) refers to each per unit increase. HF, heart failure; HR, hazard ratio; TAPSE/PASP, tricuspid annular plane systolic excursion/pulmonary artery systolic pressure.

patients with CA. We found that CA patients with TAPSE/PASP ratio <0.45 mm/mmHg had a significantly increased relative risk of all-cause mortality or HF hospitalization and of all-cause mortality. In an additional analysis, we showed that RV to PA coupling was also associated with cardiovascular death and HF hospitalization as individual endpoints.

Patients with a worse TAPSE/PASP ratio presented higher hs-TnT and NT-proBNP levels, greater LV thickness, and worse LV systolic and diastolic function suggesting a more severe cardiac involvement. At the most advanced stage, both TAPSE and PASP may decline, and therefore, their ratio may not be sensitive, at least theoretically, to detect this more advanced stage. However, also using quintiles, patients in the lowest quintile seem to have the most advanced stage. Our results are consistent with previous findings showing the prognostic value of parameters related with HF severity. Even if related to measurements of cardiac function, TAPSE/PASP ratio was an independent predictor of poor prognosis even after including in the multivariable model biomarkers (e.g. hs-TnT and NT-proBNP) or echocardiographic parameters (e.g. LV-GLS) that are well-established predictors of prognosis.

Our data are consistent with the literature with respect to the prognostic role of RV function as TAPSE was independently associated with outcomes also in our study. Among 74 patients with biopsy-proven AL-CA, Ghio *et al.*<sup>7</sup> showed that RV dysfunction, defined as TAPSE <17 mm, was associated with more severe involvement of the LV, higher NT-proBNP, and worse survival. The prognostic role of RV dysfunction was then confirmed among 82 patients with CA (AL,  $n=26$ ; variant transthyretin, ATTRv,  $n=37$ ; and wild-type, ATTRwt,  $n=19$ ).<sup>6</sup> The role of TAPSE/PASP ratio has been recently investigated among 71 patients (mean age,  $62 \pm 8$  years, 69% male) diagnosed with AL-CA. In this cohort, the time-dependent ROC and the AUC showed that the TAPSE/PASP ratio was a better predictor of short-term outcome than TAPSE or PASP.<sup>28</sup> On the other hand, in a previous study including 906 patients with ATTR-CA, TAPSE/PASP ratio was not significantly associated with the risk of all-cause death.<sup>29</sup> We found that TAPSE/PASP ratio was associated with outcome in both AL- and ATTR-CA patients, though the prognostic impact of TAPSE/PASP ratio was even more evident in AL-CA patients. Additionally, the TAPSE/PASP ratio and the 0.45 mm/mmHg cut-off better reclassified the risk over the baseline model than TAPSE or PASP alone. Therefore, the relationship between TAPSE and PASP provides a more comprehensive non-invasive measurement than each variable considered separately.<sup>7,12,30,31</sup>

## Limitations

This is a retrospective observational study, and confounding factors may have affected the results, despite extensive adjustment. A complete echocardiographic evaluation of RV function including RV longitudinal strain, fractional area change, and 3D ejection fraction was not available for the totality of patients. Moreover, there was not a core echocardiographic laboratory, but echocardiographic data have been evaluated at each centre by dedicated and highly experienced operators.

Finally, cardiovascular mortality and HF hospitalizations would be the most accurate endpoints as patients with AL-CA could also die for different causes (i.e. sepsis, pneumonia). However, cause of death was, in a meaningful proportion of cases died out of the hospital, difficult to ascertain. Thus, we analysed cardiovascular death only in an exploratory analysis. We are confident that the significance of our results could have only increased entering cardiovascular mortality rather than all-cause mortality.

## Conclusion

The TAPSE/PASP ratio was a strong and independent predictor of outcome in patients with CA. A TAPSE/PASP ratio <0.45 mm/mmHg independently predicts all-cause death or HF hospitalization and all-cause death alone with a two-fold increase in risk in the patients with lower values. Assessment of RV pulmonary pressure coupling provides a more comprehensive information about right heart performance than either TAPSE or PASP alone.

## Supplementary data

Supplementary data are available at *European Heart Journal - Cardiovascular Imaging* online.

## Funding

None declared.

**Conflict of interest:** None declared.

## Data availability

The data underlying this article will be shared on reasonable request to the corresponding author.

## References

- Garcia-Pavia P, Rapezzi C, Adler Y, Arad M, Basso C, Brucato A et al. Diagnosis and treatment of cardiac amyloidosis. A position statement of the European Society of Cardiology Working Group on Myocardial and Pericardial Diseases. *Eur J Heart Fail* 2021;**23**:512–26.
- Merlo M, Pagura L, Porcari A, Cameli M, Vergaro G, Musumeci B et al. Unmasking the prevalence of amyloid cardiomyopathy in the real world: results from Phase 2 of the AC-TIVE study, an Italian nationwide survey. *Eur J Heart Fail* 2022;**24**:1377–86.
- Tomasoni D, Aimo A, Merlo M, Nardi M, Adamo M, Bellicini MG et al. Value of the HFA-PEFF and H2 FPEF scores in patients with heart failure and preserved ejection fraction caused by cardiac amyloidosis. *Eur J Heart Fail* 2022;**24**:2374–86.
- Jurcuț R, Onciul S, Adam R, Stan C, Coriu D, Rapezzi C et al. Multimodality imaging in cardiac amyloidosis: a primer for cardiologists. *Eur Heart J Cardiovasc Imaging* 2020;**21**: 833–44.
- Aimo A, Tomasoni D, Porcari A, Vergaro G, Castiglione V, Passino C et al. Left ventricular wall thickness and severity of cardiac disease in women and men with transthyretin amyloidosis. *Eur J Heart Fail* 2023;**25**:510–4.
- Bodez D, Ternacle J, Guellich A, Galat A, Lim P, Radu C et al. Prognostic value of right ventricular systolic function in cardiac amyloidosis. *Amyloid* 2016;**23**:158–67.
- Ghio S, Perlini S, Palladini G, Marsan NA, Faggiano G, Vezzoli M et al. Importance of the echocardiographic evaluation of right ventricular function in patients with AL amyloidosis. *Eur J Heart Fail* 2007;**9**:808–13.
- Guazzi M, Bandera F, Pelissero G, Castelvécchio S, Menicanti L, Ghio S et al. Tricuspid annular plane systolic excursion and pulmonary arterial systolic pressure relationship in heart failure: an index of right ventricular contractile function and prognosis. *Am J Physiol Heart Circ Physiol* 2013;**305**:H1373–81.
- Bosch L, Lam CSP, Gong L, Chan SP, Sim D, Yeo D et al. Right ventricular dysfunction in left-sided heart failure with preserved versus reduced ejection fraction. *Eur J Heart Fail* 2017;**19**:1664–71.
- Tello K, Wan J, Dalmer A, Vanderpool R, Ghofrani HA, Naeije R et al. Validation of the tricuspid annular plane systolic excursion/systolic pulmonary artery pressure ratio for the assessment of right ventricular-arterial coupling in severe pulmonary hypertension. *Circ Cardiovasc Imaging* 2019;**12**:e009047.
- Lyhne MD, Kabrhel C, Giordano N, Andersen A, Nielsen-Kudsk JE, Zheng H et al. The echocardiographic ratio tricuspid annular plane systolic excursion/pulmonary arterial systolic pressure predicts short-term adverse outcomes in acute pulmonary embolism. *Eur Heart J Cardiovasc Imaging* 2021;**22**:285–94.
- Guazzi M, Dixon D, Labate V, Beussink-Nelson L, Bandera F, Cuttica MJ et al. RV contractile function and its coupling to pulmonary circulation in heart failure with preserved ejection fraction: stratification of clinical phenotypes and outcomes. *JACC Cardiovasc Imaging* 2017;**10**(10 Pt B):1211–21.
- Santas E, Palau P, Guazzi M, de la Espriella R, Minana G, Sanchis J et al. Usefulness of right ventricular to pulmonary circulation coupling as an indicator of risk for recurrent admissions in heart failure with preserved ejection fraction. *Am J Cardiol* 2019;**124**:567–72.
- Sugiura A, Kavsar R, Spieker M, Iliadis C, Mauri V, Tanaka T et al. Impact of right ventricular-pulmonary arterial coupling on clinical outcomes of tricuspid regurgitation. *EuroIntervention* 2022;**18**:852–61.
- Brener MI, Lurz P, Hausleiter J, Rodés-Cabau J, Fam N, Kodali SK et al. Right ventricular-pulmonary arterial coupling and afterload reserve in patients undergoing transcatheter tricuspid valve repair. *J Am Coll Cardiol* 2022;**79**:448–61.
- Brener MI, Grayburn P, Lindenfeld J, Burkhoff D, Liu M, Zhou Z et al. Right ventricular-pulmonary arterial coupling in patients with HF secondary MR: analysis from the COAPT trial. *JACC Cardiovasc Interv* 2021;**14**:2231–42.
- McDonagh TA, Metra M, Adamo M, Gardner RS, Baumbach A, Böhm M et al. 2021 ESC guidelines for the diagnosis and treatment of acute and chronic heart failure: developed by the task force for the diagnosis and treatment of acute and chronic heart failure of the European Society of Cardiology (ESC), with the special contribution of the Heart Failure Association (HFA) of the ESC. *Eur J Heart Fail*. 2022;**24**:4–131.
- Kittleson MM, Maurer MS, Ambardekar AV, Bullock-Palmer RP, Chang PP, Eisen HJ et al. Cardiac amyloidosis: evolving diagnosis and management: a scientific statement from the American Heart Association. *Circulation* 2020;**142**:e7–22.
- Lang RM, Badano LP, Mor-Avi V, Filalo J, Armstrong A, Ernande L et al. Recommendations for cardiac chamber quantification by echocardiography in adults: an update from the American Society of Echocardiography and the European Association of Cardiovascular Imaging. *Eur Heart J Cardiovasc Imaging* 2015;**16**:233–70.
- Nakagawa A, Yasumura Y, Yoshida C, Okumura T, Tateishi J, Yoshida J et al. Prognostic importance of right ventricular-vascular uncoupling in acute decompensated heart failure with preserved ejection fraction. *Circ Cardiovasc Imaging* 2020;**13**:e011430.
- Adamo M, Maccagni G, Fiorina C, Giannini C, Angelillis M, Costa G et al. Prognostic value of right ventricle to pulmonary artery coupling in transcatheter aortic valve implantation recipients. *J Cardiovasc Med (Hagerstown)* 2022;**23**:615–22.
- Leurent G, Auffret V, Donal E. Right ventricular-pulmonary artery coupling: a simple marker to guide complex clinical decisions? *JACC Cardiovasc Interv* 2022;**15**:1834–6.
- Cahill TJ, Pibarot P, Yu X, Babaliaros V, Blanke P, Clavel MA et al. Impact of right ventricle-pulmonary artery coupling on clinical outcomes in the PARTNER 3 trial. *JACC Cardiovasc Interv* 2022;**15**:1823–33.
- Adamo M, Inciardi RM, Tomasoni D, Dallapellegrina L, Estevez-Loureiro R, Stolfo D et al. Changes in right ventricular-to-pulmonary artery coupling after transcatheter edge-to-edge repair in secondary mitral regurgitation. *JACC Cardiovasc Imaging* 2022;**15**:2038–47.
- Stretti L, Zippo D, Coats AJS, Anker MS, von Haehling S, Metra M et al. A year in heart failure: an update of recent findings. *ESC Heart Fail* 2021;**8**:4370–93.
- González-López E, Gallego-Delgado M, Guzzo-Merello G, de Haro-Del Moral FJ, Cobo-Marcos M, Robles C et al. Wild-type transthyretin amyloidosis as a cause of heart failure with preserved ejection fraction. *Eur Heart J* 2015;**36**:2585–94.
- Aimo A, Merlo M, Porcari A, Georgiopoulos G, Pagura L, Vergaro G et al. Redefining the epidemiology of cardiac amyloidosis. A systematic review and meta-analysis of screening studies. *Eur J Heart Fail* 2022;**24**:2342–51.
- Yu F, Cui Y, Shi J, Wang L, Zhou Y, Ye T et al. Association between the TAPSE to PASP ratio and short-term outcome in patients with light-chain cardiac amyloidosis. *Int J Cardiol* 2023:131108. doi: 10.1016/j.ijcard.2023.05.058.
- Bandera F, Martone R, Chacko L, Ganesanathan S, Gilbertson JA, Ponticos M et al. Clinical importance of left atrial infiltration in cardiac transthyretin amyloidosis. *JACC Cardiovasc Imaging* 2022;**15**:17–29.
- Ghio S, Guazzi M, Scardovi AB, Klersy C, Clemenza F, Carluccio E et al. Different correlates but similar prognostic implications for right ventricular dysfunction in heart failure patients with reduced or preserved ejection fraction. *Eur J Heart Fail* 2017;**19**:873–9.
- Guazzi M, Naeije R, Arena R, Corrà U, Ghio S, Forfia P et al. Echocardiography of right ventriculoarterial coupling combined with cardiopulmonary exercise testing to predict outcome in heart failure. *Chest* 2015;**148**:226–34.